



Research Article

# An Investigation on the Structural, Optical and Corrosion Behavior of Different Al/Graphene Nano Composite Material

Akash Singh<sup>1</sup>, Suraj Singh<sup>2</sup>, Amrendra Singh<sup>3</sup> and Shashank Dubey<sup>4</sup>

<sup>1,2,3</sup>Mechanical Engineering Department, Uma Nath Singh Institute of Engineering & Technology, V.B.S. Purvanchal University, Jaunpur, Uttar Pradesh, India.

<sup>4</sup>Assistant Professor, Mechanical Engineering Department, Uma Nath Singh Institute of Engineering & Technology, V.B.S. Purvanchal University, Jaunpur, Uttar Pradesh, India.

Corresponding author email: shashank.dubey001@gmail.com

**ABSTRACT:** An innovative approach to materials engineering, aluminium-graphene nanocomposites have great promise for cutting-edge technological applications. This study carefully looks into the many performance aspects of aluminium matrix composites that have been improved with graphene nanoparticles, with a focus on their structural integrity, optical properties, and resistance to corrosion. In this study, aluminum-graphene nanocomposites with graphene concentrations ranging from 0.5 to 1.25 weight percent are created using sophisticated powder metallurgical processes. X-ray diffraction (XRD), Fourier transform infrared (FTIR) spectroscopy, field emission scanning electron microscopy (FE-SEM), energy dispersive X-ray analysis (EDXA), and ultraviolet-visible (UV-vis) spectroscopy were used to characterize the as-prepared nanocomposites. We conduct a thorough analysis of the interfacial interactions and microstructural changes between graphene and aluminium nanosheets. Important results show notable increases in mechanical characteristics, with graphene reinforcement showing notable gains in microstructural integrity. Interestingly, composites with 0.5 weight percent graphene concentration performed best; over this point, material properties are adversely affected by graphene aggregation. The improved mechanical characteristics of the composite are further increased by the production of nano-sized aluminium carbides ( $Al_4C_3$ ) at the aluminum-graphene interface. Additionally, the study examines the optical properties and corrosion behaviour of these nanocomposites, emphasizing their potential uses in advanced structural components, heat management, and aerospace. This work offers important insights into the design and optimization of aluminum-graphene nanocomposite materials by methodically examining the complex interactions between graphene concentrations, processing factors, and material performance.

**KEYWORDS:** Al-doped Graphene, Nanocomposite, Metal Matrix, Conductivity, Characterization, Alloy.

## INTRODUCTION

Aluminum (Al) and its alloys have been crucial in industries such as automotive and aerospace due to their lightweight properties, excellent corrosion resistance, and high strength-to-weight ratio. However, the demand for advanced materials with superior mechanical, thermal, and electrical properties has driven interest in the development of aluminum-based composites. Among these, aluminum/graphene nanocomposites (Al/Gr NCs) have emerged as a promising category. Graphene, a two-dimensional carbon allotrope, exhibits exceptional mechanical

strength, a high specific surface area, and excellent thermal and electrical conductivity, making it an outstanding reinforcing material for metal matrices [1]. When incorporated into aluminum composites, graphene not only enhances mechanical properties but also introduces unique functional attributes, such as improved optical performance and greater corrosion resistance. These advancements have positioned Al/Gr NCs as a focal point for research on next-generation materials tailored for demanding industrial applications. This study explores the structural, optical, and corrosion characteristics of various Al/Gr nanocomposites [2]. By systematically varying synthesis parameters, graphene content, and processing techniques, it seeks to establish correlations between microstructural features and material performance.

Gaining a deeper understanding of these relationships is essential for optimizing the design and fabrication of Al/Gr nanocomposites to meet specific application demands. The research begins with a detailed analysis of the structural features of Al/Gr nanocomposites using advanced techniques such as scanning electron microscopy (SEM), and X-ray diffraction (XRD). These methods provide insights into interfacial bonding, graphene dispersion within the aluminum matrix, and microstructural evolution during processing [3-4]. Spectroscopic techniques are employed to study the optical properties of the composites, which hold significance for applications in photonics and energy harvesting. Finally, the corrosion resistance of the materials is evaluated under various environmental conditions to assess their suitability for harsh and corrosive environments. This comprehensive investigation aims to address knowledge gaps in understanding the structure-property relationships of Al/Gr nanocomposites. The findings are expected to contribute to the advancement of high-performance aluminum-based materials, supporting the development of lightweight, durable, and multifunctional components for a range of industrial applications.

## MATERIALS AND EXPERIMENTAL METHODS

### *Chemicals and Materials*

Graphite flakes with a 325 mesh size, sourced from Alfa Aesar, were utilized to synthesize graphene oxide (GO). Chemicals including sulfuric acid (H<sub>2</sub>SO<sub>4</sub>, 98%), potassium permanganate (KMnO<sub>4</sub>, 99.9%), hydrogen peroxide (H<sub>2</sub>O<sub>2</sub>, 30%), and sodium nitrate (NaNO<sub>3</sub>) were obtained from Alfa Aesar and used without further purification. Aluminum powder was also procured from Alfa Aesar and used as received. Distilled water and ethanol were employed throughout the sample preparation process.

### *Synthesis*

The production of graphene from graphite typically involves the following steps:

1. Preparation of Graphene Oxide: Graphite (1g) was mixed with 0.5g of sodium nitrate (NaNO<sub>3</sub>) and oxidized using potassium permanganate (3g, added gradually) in 23 ml of concentrated sulfuric acid (H<sub>2</sub>SO<sub>4</sub>). This process introduces oxygen-containing functional groups to the graphene surface, making it hydrophilic. The mixture was stirred in an ice bath for one hour, followed by the addition of 140 ml of deionized water and 5 ml of hydrogen peroxide (H<sub>2</sub>O<sub>2</sub>). The reaction was then stirred for an additional three hours.
2. Reduction of Graphene Oxide: To restore the sp<sup>2</sup> carbon-carbon bonding and remove the oxygen-containing functional groups, the graphene oxide was reduced. This was achieved by mixing the graphene oxide with a reducing agent (2g of sodium borohydride) in ethanol. The mixture was stirred to ensure uniform dispersion of the graphene oxide and then heated to a temperature range of 70°C to 100°C to initiate the reduction process.

3. Exfoliation of Graphene: The reduced graphene oxide was subjected to mechanical shearing for two hours to separate the graphene sheets. The exfoliated graphene sheets were then dispersed in a solvent.
4. Purification of Graphene: To remove impurities such as unreacted graphene oxide, residual oxidizing agents, or metallic catalysts, the graphene sheets were thoroughly washed with ethanol and deionized water. Finally, the material was filtered and dried at 70°C to obtain purified graphene as represented in Figure 1(a) and 1(b).

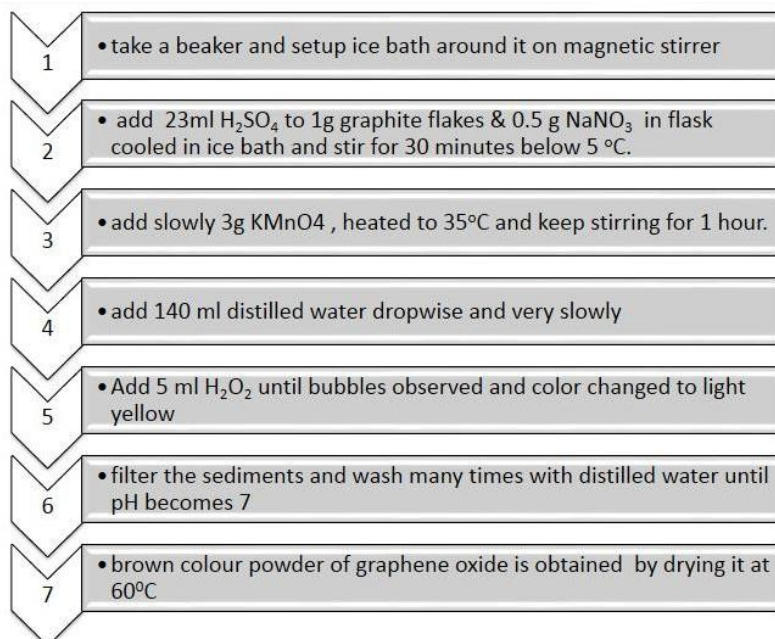


**Figure 1(a): Synthesis of graphene oxide by Hummer's method.**

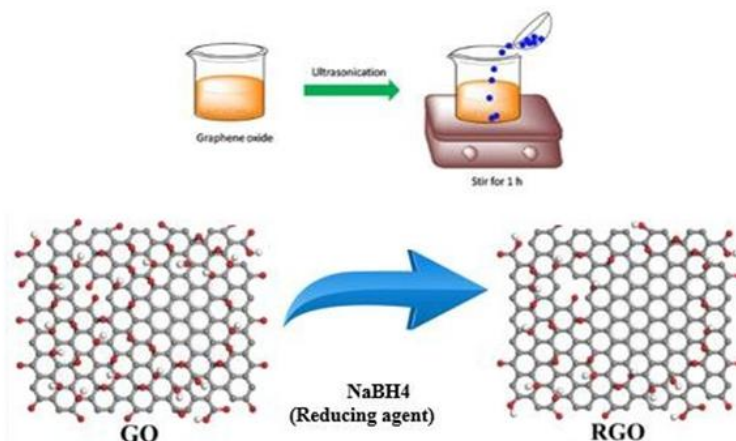


**Figure 1(b): Reduction of GO to graphene.**

#### *Fabrication of Al-RGO Composite*

In this study, the Al-RGO nanocomposite material was fabricated using the powder metallurgy method as shown in Figure 2. The ball milling technique was employed to mix reduced graphene oxide (RGO) powder with aluminum powder. Different weight percentages of RGO (0.5, 0.75, 1.00, and 1.25 wt%) were combined with aluminum powder in a ball mill at room temperature for 3 hours, using steel balls with a ball-to-powder ratio of 20:1 as shown in Table

1. To eliminate impurities, the samples were further dried at 80°C for 10 hours. The processed materials were then subjected to additional milling in a planetary ball mill for 3 hours at a rotational speed of 250 rpm [5]. After milling, the resulting mixture was transferred to a vacuum drying oven to obtain the final mixed powders.

**Table 1: Experimental data used in the synthesis of Al/RGO.**

Samples Name	S1	S2	S3	S4
rGO per total content (wt%)	0.5	0.75	1.00	1.25
Al per total content (wt %)	99.5	99.25	99.00	98.75



**Figure 2: Illustration of detailed processing of RGO.**

## RESULTS AND DISCUSSIONS

### Characterization

Figure 3 and 4 show the scanning electron microscopy (SEM) & EDS of pure grapheme which is prepared by the modified hummer’s method EDS graph shows 99.7% carbon. Figures 5 and 6 illustrate the morphological structure of the Al-RGO composite powder following the ball milling process.

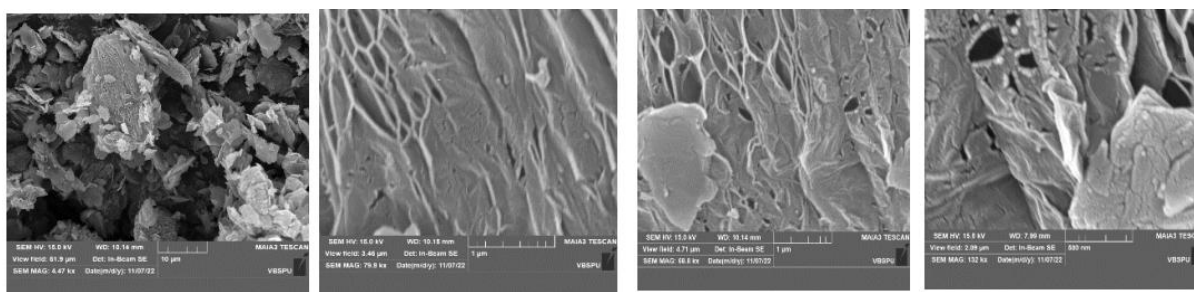


**Figure 3: Scanning electron microscopy (SEM): (a-d) of pure graphene.**

The reduced graphene oxide (RGO) sheets are visible on the aluminum powder particles, with curled and wrinkled RGO sheets covering the surfaces of the aluminum particles, as shown in

the magnified SEM image. This finding suggests that graphene can effectively reinforce aluminum. The SEM images of aluminum matrix composite (AMC) powders with graphene sheets revealed the distribution of the reinforcement phase on the aluminum particles. However, the adsorption of graphene sheets onto the aluminum particles was minimal, with most graphene sheets observed adjacent to the aluminum powder particles [6].

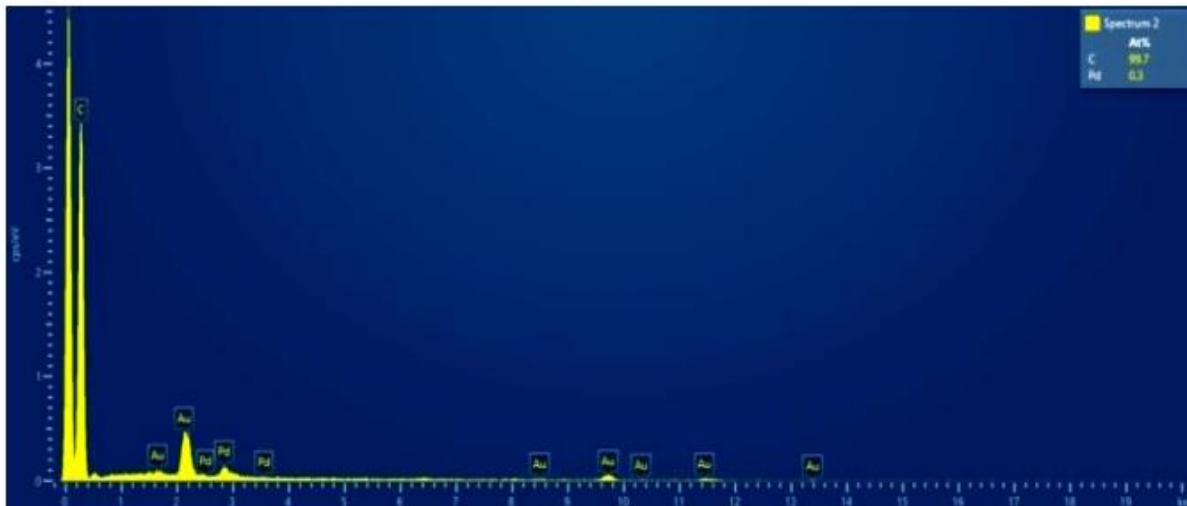


Figure 4: EDS of pure graphene.

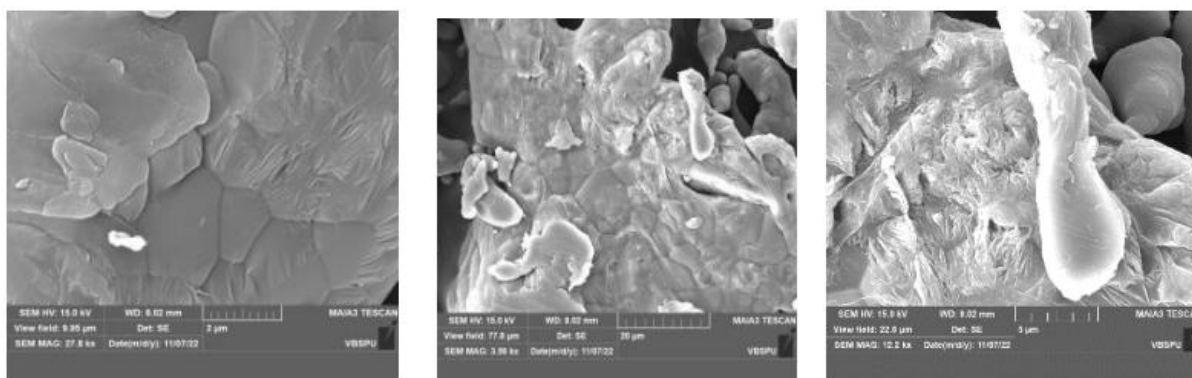


Figure 5: (SEM): (a-c) of graphene/Al nanocomposite samples.



Figure 6: EDS of graphene/Al nanocomposite samples.

The FT-IR analysis confirms the presence of various functional groups bonded to the Al/Graphene nanocomposite material. The FT-IR spectrum of pure graphene, shown in Figure 9, exhibits a peak at  $3910\text{ cm}^{-1}$ , corresponding to the stretching vibration of free O-H groups from hydroxyl functional groups. The weak intensity of this peak, along with the absence of significant peaks in the  $3000\text{--}3700\text{ cm}^{-1}$  range, indicates a low concentration of adsorbed water molecules within the graphene structure [7-9]. Peaks observed at  $1238\text{ cm}^{-1}$  and  $1698\text{ cm}^{-1}$  are attributed to the C=O stretching vibrations of carboxyl and carbonyl groups located at the edges of the reduced graphene oxide (RGO).

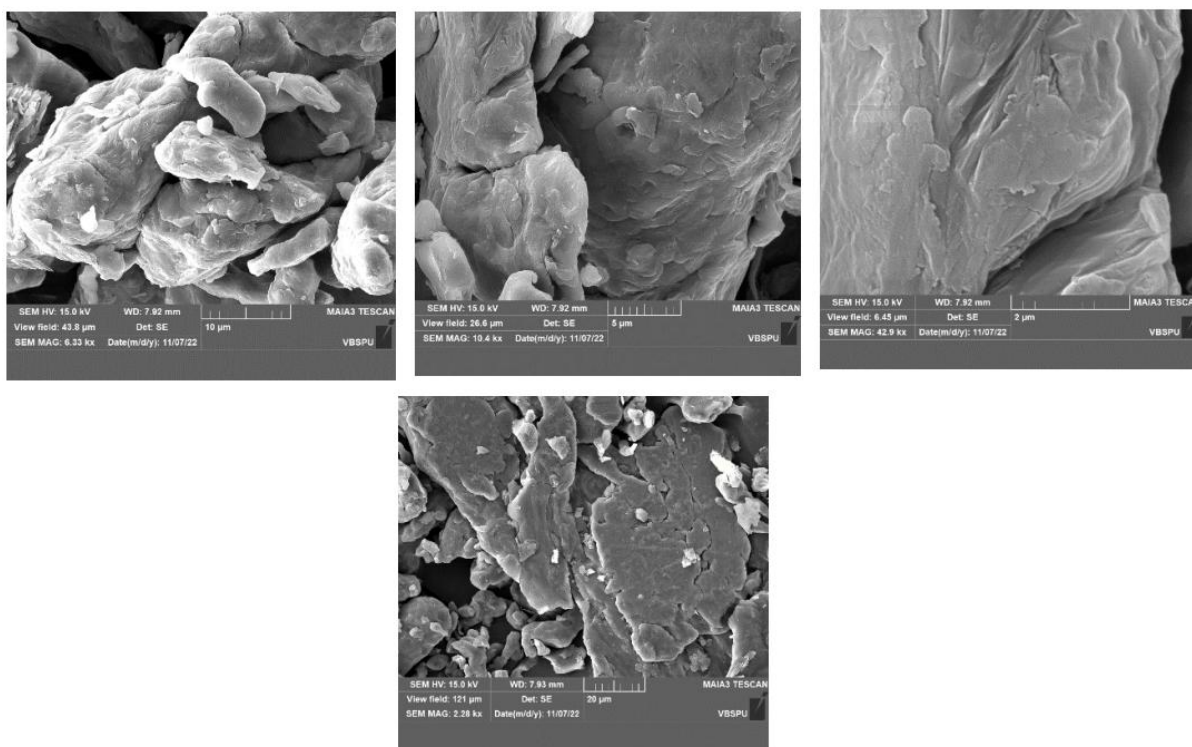


Figure 7: Scanning electron microscopy (SEM): (a-d) of graphene/Al by ball milling.



Figure 8: EDS of graphene/Al by ball milling.

Additionally, the peaks at  $1647\text{ cm}^{-1}$  and  $1527\text{ cm}^{-1}$  correspond to the stretching vibrations of aromatic C=C bonds, representing carbon atoms that remain functionalized during oxidation. The strong signal at  $3500\text{ cm}^{-1}$  in the RGO spectrum is associated with O-H stretching

vibrations from hydroxyl groups and adsorbed water molecules [10]. Figure 10 (a & b) presents the FTIR spectra of composite powders prepared using the wet method and ball milling of Al and RGO powders. The spectra of the composite powders reveal two additional peaks at  $1461\text{ cm}^{-1}$  and  $3418\text{ cm}^{-1}$ , corresponding to the stretching vibrations of free O-H bonds and the bending vibrations of C-OH bonds, respectively [11].

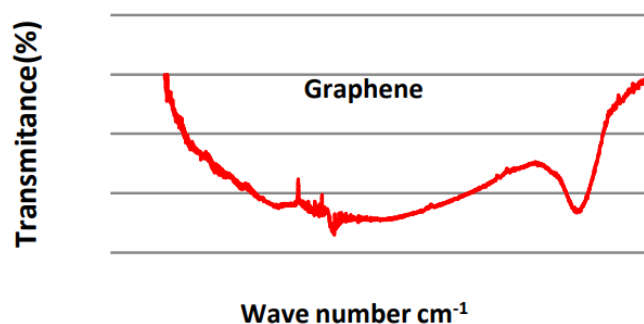


Figure 9: FT-IR spectra of graphene.

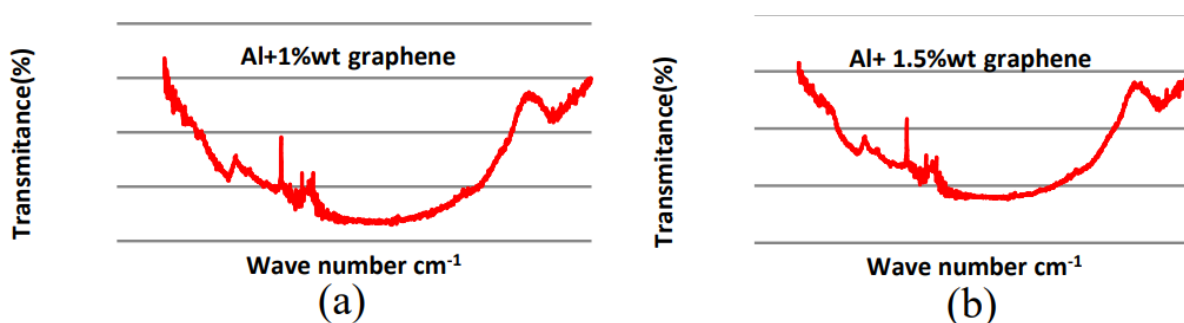


Figure 10: FT-IR spectra of aluminium- graphene nanocomposite powder of graphene/Al.

#### *Corrosion Resistance Performance*

Impedance and polarization tests were utilized to evaluate the corrosion resistance properties. Figure 11 illustrates the Nyquist and Tafel polarization curves of the graphene/Al composites. The polarization curve was used to derive the  $E_{\text{corr}}$  and  $I_{\text{corr}}$  values, as shown in Table 2. The Nyquist curve, commonly employed to evaluate system stability, typically appears as a semicircle or a series of connected semicircles. The Nyquist curves for all graphene/Al composites displayed significantly larger diameters compared to the pure aluminum sample, which was used as a reference (Figure 11a). This indicates that the corrosion-resistant stability of graphene/Al composites in a 3.5 wt% NaCl solution improves with increasing graphene content. This behavior is attributed to the electrode-electrolyte interface, where the hydrophobic nature of graphene enhances the Nyquist curves by improving the contact interface between aluminum and the corrosive solution [12–14]. However, an excessive amount of graphene reduces the Nyquist radii, which can be explained by graphene agglomeration. This aggregation diminishes the barrier effect, reducing the contact-blocking ability between aluminum and the corrosive solution. Additionally, the excellent electrical conductivity of graphene may contribute to decreased corrosion resistance stability.

All prepared samples of pure aluminum and graphene/Al composites exhibit a passivation state, as illustrated in Figure 11(b). This behavior is attributed to the rapid formation of an oxide

film or a corrosion product layer on the aluminum matrix after it is penetrated, effectively preventing further corrosion. Pure aluminum demonstrates the highest pitting resistance and susceptibility, while the graphene/Al composites exhibit comparatively lower values. This is evident from the lower breakdown onset of the passive films in the graphene/Al composites compared to pure aluminum. The corrosion resistance of each sample is assessed through the  $E_{corr}$  and  $I_{corr}$  values.

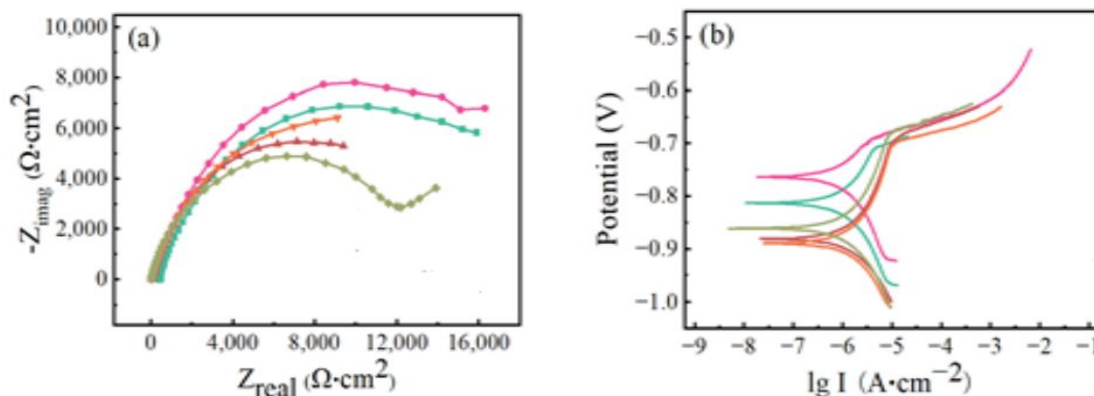


**Figure 11. (a) Nyquist plots of graphene/Al composites, (b) potentiodynamic polarization curves of graphene/Al composites.**

As shown in Figure 11(b), both pure aluminum and graphene/Al composites form oxide films or corrosion product layers that halt further corrosion. However, the graphene/Al composites show reduced pitting resistance and susceptibility compared to pure aluminum, as indicated by the earlier breakdown of their passive films. Despite this, the  $E_{corr}$  values for the 1.00 wt% and 1.25 wt% graphene/Al composites exceed those of pure aluminum, even with a small addition of graphene. Among all the composite samples, the 1.25 wt% graphene/Al composite exhibits the highest  $E_{corr}$  value, indicating superior thermodynamic corrosion resistance [18-19]. Notably, the relationship between  $E_{corr}$  and  $I_{corr}$  is non-linear, further emphasizing the influence of graphene content on corrosion resistance.

**Table 2. Corrosion potential ( $E_{corr}$ ) & corrosion current density ( $I_{corr}$ ) of the pure aluminum sample and graphene/Al composites.**

Sl. No.	Sample	$E_{corr}$ (mV)	$I_{corr}$ ( $\mu A/cm^2$ )
1	Al	-851.4	2.356
2	S1 (Al-0.5 wt% Gr)	-823.6	3.011
3	S2 (Al-0.75 wt% Gr)	-753.8	2.508
4	S3 (Al-1.0 wt% Gr)	-871.4	3.151
5	S4 (Al-1.25 wt% Gr)	-889.5	3.582

The  $I_{corr}$  values of all graphene/Al composites are higher than those of the pure aluminum sample, aligning with previous corrosion studies on graphene-reinforced aluminum composites and pure aluminum. One contributing factor to this increased  $I_{corr}$  is the lower densification of the graphene/Al composites compared to pure aluminum. The porosity and cracks at the interface between the graphene reinforcement and the aluminum matrix facilitate metal pitting

and the dissolution of the aluminum matrix [20]. Additionally, the high density of aluminum oxide serves as a protective barrier, preventing further corrosion. However, graphene's loosely layered structure and its dispersion within the aluminum matrix can disrupt the continuity of the aluminum oxide layer in certain regions. This disruption creates conditions that allow further corrosion to propagate within the aluminum matrix, increasing the number of corrosion sites [21].

## CONCLUSION

This study provides a comprehensive analysis of the optical, corrosion, and structural properties of aluminum/graphene nanocomposites, shedding light on the potential of these advanced materials. The research underscores the significance of graphene content and its dispersion in influencing the microstructural features and overall performance of the composites. Key findings reveal the synergistic improvement in mechanical, optical, and corrosion resistance properties achieved by incorporating graphene into the aluminum matrix. The structural analysis highlights the importance of strong interfacial bonding and uniform graphene distribution, which play a critical role in enhancing the composites' stability and mechanical integrity. Optical characterization demonstrated promising improvements in thermal and photonic responses, paving the way for applications in energy-efficient devices. The enhanced corrosion resistance of Al/graphene nanocomposites further broadens their industrial applicability, making them suitable for use in chemically aggressive environments. The findings emphasize the need to refine processing techniques and optimize synthesis parameters to fully harness the benefits of graphene reinforcement. Future studies should focus on advancing manufacturing methods, exploring alternative graphene derivatives, and evaluating long-term performance under real-world conditions. This research lays a solid foundation for developing next-generation aluminum-based materials that meet the rigorous demands of modern engineering applications by deepening our understanding of the structure-property relationships. In conclusion, aluminum/graphene nanocomposites represent a versatile, high-performance material system with the potential to revolutionize industries reliant on strong, lightweight, and multifunctional components. Continued research in this area is expected to drive innovation and open new pathways for the advancement of sophisticated materials.

## REFERENCES

- [1] Y. Li, Y.H. Zhao, V. Ortalan, W. Liu, Z.H. Zhang, R.G. Vogt, N.D. Browning, E.J. Lavernia, and J.M. Schoenung, Investigation of aluminum-based nanocomposites with ultra-high strength, *Mater. Sci. Eng. A*, 527(2009), No. 1-2, p. 305.
- [2] Bai Y, Han E H, Tan R B. Research on properties of Aluminum matrix composites[J]. *Materials Protection*, 2003, 36(9):5-7.
- [3] M. Sharma and V. Sharma, Chemical, mechanical, and thermal expansion properties of a carbon nanotube-reinforced aluminum nanocomposite, *Int. J. Miner. Metall. Mater.* 23 (2016), No.2, p. 222.
- [4] Zhang S. Y., Meng F. Q, Chen Y. Y, et al. Research progress of metal matrix composites reinforced with particles[J]. *Materials Review*, 1996, 10(2): 66-71.
- [5] Jiang S H, Wang H H, Yuan H B, et al. The feature of MMCs and its prospects of application in engineering[J]. *Automobile Science and Technology*, 2002, (6):21-24.
- [6] Gupta A, Chen G, Joshi P, et al. Raman scattering from high- frequency phonons in supported n-graphene layer films[J]. *Nano Letters*, 2006, 6(12): 2667-2673.

- [7] J. Hwang, T. Yoon, S.H. Jin, J. Lee, T.S. Kim, S.H. Hong, and S. Jeon, Enhanced mechanical properties of graphene/copper nanocomposites using a molecular-level mixing process, *Adv. Mater.*, 25(2013), No. 46, p. 6724.
- [8] Zhou, W.; Mikulova, P.; Fan, Y.; Kikuchi, K.; Nomura, N.; Kawasaki, A. Interfacial reaction induced efficient load transfer in few-layer graphene reinforced Al matrix composites for high-performance conductor. *Compos. Part B Eng.* 2019, 167, 93–99.
- [9] Chen, W.; Yang, T.; Dong, L.; Elmasry, A.; Song, J.; Deng, N.; Elmarakbi, A.; Liu, T.; Lv, H.B.; Fu, Y.Q. Advances in graphene reinforced metal matrix nanocomposites: Mechanisms, processing, modelling, properties and applications. *Nanotechnol. Precis.Eng.* 2020, 3, 189–210.
- [10] Luo H. Research on the Microstructure and Properties of Graphene Nanoplatelets Reinforced Aluminum Matrix Composites [D]. Harbin: Harbin Institute of Technology, 2015.
- [11] Khan, M.; Din, R.U.; Basit, M.A.; Wadood, A.; Husain, S.W.; Akhtar, S.; Aune, R.E. Study of microstructure and mechanical behaviour of aluminium alloy hybrid composite with boron carbide and graphene nanoplatelets. *Mater. Chem. Phys.* 2021, 271,124936.
- [12] Liu J, Umar K, Jonathan C, et al. Graphene oxide and graphene nanosheet reinforced aluminium matrix composites: powder synthesis and prepared composite characteristics[J]. *Materials and Design*, 2016, 94:87-94.
- [13] Wang J, Li Z, Fan G, et al. Reinforcement with graphene nanosheets in aluminum matrix composites[J]. *Scripta Materialia*, 2012, 66(8):594-597.
- [14] Rashad, M.; Pan, F.; Yu, Z.; Asif, M.; Lin, H.; Pan, R. Investigation on microstructural, mechanical and electrochemical properties of aluminum composites reinforced with graphene nanoplatelets. *Prog. Nat. Sci.* 2015, 25, 460–470.
- [15] Krishnamoorthy K, Jeyasubramanian K, Premanathan M, et al. Graphene oxide nanopaint[J]. *Carbon*, 2014, 72:328-337.
- [16] Prasai D, Tuberquia J.C, Harl R.R, et al. Graphene:corrosion-inhibiting coating[J]. *ACS Nano*, 2012, 6:1102-1108.
- [17] Hikku G. S, Jeyasubramanian K, Rahul G, et al. Corrosion resistance behaviour of graphene/polyvinyl alcohol nanocomposite coating for aluminium-2219 alloy[J]. *Journal of Alloys and Compounds*, 2017, 716:259-269.
- [18] Prakash, C.; Singh, S.; Sharma, S.; Garg, H.; Singh, J.; Kumar, H.; Singh, G. Fabrication of aluminium carbon nano tube silicon carbide particles-based hybrid nano-composite by spark plasma sintering. *Mater. Today Proc.* 2020, 21, 1637–1642.
- [19] Porwal H, Tatarko P, Grasso S, et al. Graphene reinforced alumina nano-composites[J]. *Carbon*, 2013, 64(11):359-369.
- [20] Francois L, Jerome W, Thiebaud R. Hall patch law revisited in terms of collective dislocation dynamics[J]. *Physical Review Letters*, 2006, 97(7):75504-75505.
- [21] Lefebvre S, Devincre B, Hoc T. Yield stress strengthening in ultrafine grained metals: A two-dimensional simulation of dislocation dynamics[J]. *Journal of the Mechanics and Physics of Solids*, 2007, 55(4):788-802.



This is an open access article distributed under the terms of the Creative Commons NC-SA 4.0 License Attribution—unrestricted use, sharing, adaptation, distribution and reproduction in any medium or format, for any purpose non-commercially. This allows others to remix, tweak, and build upon the work non-commercially, as long as the author is credited and the new creations are licensed under the identical terms. For any query contact: [research@ciir.in](mailto:research@ciir.in)